OVER-BARRIER DECAY OF A MIXED STATE IN 2D MULTIWELL POTENTIALS

YU.L. BOLOTIN, V.A. CHERKASKIY, G.I. IVASHKEVYCH, A.I. KIRDIN

National Scientific Center "Kharkov Institute of Physics and Technology"
(1, Akademicheskaya Str., Kharkov 61108, Ukraine; e-mail: bolotin@kipt.kharkov.ua)

PACS 05.45.Ac, 05.45.Pq

The classical escape in 2D Hamiltonian systems with a mixed state has been studied numerically and analytically. The wide class of potentials with a mixed state is presented by polynomial potentials. In potentials, where the mixed state could be realized, i.e. the configuration space contains regions of both regular and chaotic motions, the escape problem has a number of new features. In particular, some local minima become a trap with the number of particles depending on the energy and other values that characterize the ensemble of particles. Choosing a form of the initial ensemble, one chooses the set of parameters that determine the number of trapped particles.

1. Introduction

Chaotic dynamics is the most common way of the evolution of nonlinear systems [1]. Examples of dynamic chaos were discovered almost in every branch of physics, and their number continuously increases. Recently, the well-defined trend has emerged in the research of dynamic chaos: the transition from a trivial demonstration of chaos to the study of its manifestations in specific physical systems. In the present paper, we discuss the influence of chaos on the escape of trajectories from localized regions of the phase or configuration space. Such escapes are an important topic in dynamics and describes the decay of metastable states in many areas of physics such as, for instance, chemical and nuclear reactions, atomic ionization, *etc.*

The problem has a rich history and a number of realizations in different systems. Almost a century ago, Sabine [2] had considered the diminution of sound in concert halls, and Legrand and Sornette [3] had shown later on that the problem is equivalent to the escape one. The corresponding decay rate is $\int \alpha(s)ds$, and $\alpha(s)$ is the absorption coefficient at a coordinate s of the billiard boundary, $\alpha(s) = 1$ on the opening of Δ in width, and $\alpha(s) = 0$ elsewhere.

Another application of the escape problem links to the nondestructive monitoring of a system [4]. If some system is connected to the surrounding only via a small opening in its boundary, it became possible to understand the dynamics of the system by exploring the escaping particles. So the natural question arises: how does the escape law depend on the motion? For strongly chaotic systems, the exponential decay is expected [5–7]. Bauer and Bertsch [5] considered the escape of particles through a small opening in the billiard's boundary. When exploring a regular billiard, i.e. the rectangular one without a scattering center, the power law emerges in a long time. The qualitative consideration of the mechanism of generation of power tails is given in [8].

For a rectangular billiard with circular scattering center in it, the decay of the initial ensemble of $N(0)$ particles is of exponential character. By a simple consideration, we have that the corresponding decay rate

$$N(t) = N(0)\exp(-\alpha t),\ \alpha = \frac{p\Delta}{\pi A_c}. \quad (1)$$

Here, p is the particle's momentum, Δ is the opening width, and A_c is the billiard area. We show further that the exponential decay is a common feature of purely chaotic systems.

2. Mixed State

The passage from billiards to potential systems increases the number of possible situations. A one-well potential is the simplest case for considering the escape. In [9], Kandrup *et al.* have researched the escape from three different Hamiltonian systems of the form $H = H_0 + \epsilon H'$ and made important conclusions. In particular, the exploration of the escape probability leads to the conclusion that the initial ensemble is divided into three parts. The first part consists of the trajectories that are not confined by any cantori, while the second exhibits the confinement for a quite long time. The third part (if significant) consists of regular trajectories. Thus, the escape probability saturates at some level P_0 independent of details of the initial ensemble due to the escape of unconfined trajectories and decays toward zero at later times due to the escape of initially confined chaotic trajectories. Importantly, P_0 scales as $P_0 \propto (\epsilon - \epsilon_1)^\alpha$ with

a value of perturbation, where ϵ_1 is the critical value, when the escape becomes energetically possible.

Zhao and Du [10] have explored the escape from the Henon–Heiles potential:

$$U_{\rm HH}(x,y) = \frac{x^2+y^2}{2} + xy^2 - \frac{x^3}{3}. \quad (2)$$

At the energies $E > 1/6$, a trajectory could leave the potential well through one of the three openings placed symmetrically. The numerical simulation performed by Zhao and Du has shown that the escape follows the exponential law. At over-saddle energies, the phase space with the Henon–Heiles Hamiltonian is almost homogeneous, and the motion is chaotic. Using this, the escape rate could be derived, and it fits numerical results with high accuracy. This situation is similar to the escape from chaotic billiards.

Another study of the escape from the Henon–Heiles potential was performed in [11], by focusing on the determination of the escape basins.

In contrast to billiards and the Henon–Heiles potential, some potentials have a highly inhomogeneous phase space that consists of macroscopically significant components corresponding to both regular and chaotic motions. A wide class of systems with an inhomogeneous phase space is represented by multiwell potentials. We will focus our research on the escape from such potentials. The preliminary results are presented in [12, 13]. The regularity–chaos transition in multiwell potentials has a distinctive feature which consists in the difference of critical energies in different local minima. This leads to the different (either regular or chaotic) regimes of motion in different local minima at the same energy, i.e. the ratio of chaotic trajectories in some local minimum significantly differs from the ratio in other minima. Such a kind of the dynamics is called the mixed state [14]. It is worth to mention that critical energies lie below the saddle energy, i.e. the energy, above which the local minima are no more separated.

We will demonstrate the mixed state in two representative examples of $2D$ multiwell potentials: the lower umbilical catastrophe D_5,

$$U_{D_5} = 2ay^2 - x^2 + xy^2 + \frac{1}{4}x^4 \quad (3)$$

for $a = 1.1$ and the quadrupole nuclear oscillatory potential (QO),

$$U_{\rm QO}(x,y,W) = \frac{x^2+y^2}{2W} + xy^2 - \frac{1}{3}x^3 + (x^2+y^2)^2 \quad (4)$$

for $W = 18$. The D_5 potential has two local minima and three saddles, and it is the simplest potential, where a mixed state is observed. Figure 1 shows the Poincaré sections for different energies in the considered potentials. It demonstrates the dynamical evolution in different local minima. At low energies, the motion has a well-marked quasiperiodic character in both minima. As the energy grows, the gradual regularity–chaos transition is observed. However, the changes in features of the trajectories localized in different minima are sharply distinct. In the left minimum, a significant fraction of trajectories becomes chaotic already at about a half of the saddle energy. Near the saddle energy, almost all initial conditions result in chaotic trajectories. In the right minimum at the same energy, the motion remains regular, and this situation is preserved up to the saddle energy (we call this minimum the regular one for simplicity).

Moreover, at energies above the saddle one, the phase space is still divided into chaotic and regular components, but they are not separated in the configuration space.

Earlier, we have shown that the mixed state opens new possibilities for the investigations of quantum manifestations of classical stochasticity [15]. The aim of the present work is to study the classical escape from separated local minima realizing a mixed state. We show that the escape from such local minima has all abovementioned properties of the decay of chaotic systems and also a diversity of basically new features representing an interesting topic for the conceptual understanding of the chaotic dynamics and for applications as well. We are interested in both the first passage effects and the dynamical equilibrium setup for a finite motion (for example, in the QO potential). It is important to emphasize that though we study the process of escape from a specific local minimum, the over-barrier case of the mixed state has a specific memory: the general phase space structure at supersaddle energies is determined by the characteristics of motion in all other local minima.

3. Decay of the Uniformly Distributed Ensemble

At the energies above the saddle, i.e. $E > E_S$, different components are not separated in the configuration space. Figure 2 represents the Poincaré section for the D_5 potential at a supersaddle energy. The "chaotic sea" stretches on whole accessible area, while a regular island in the right well is localized. This means that, being initially localized in the right well, chaotic trajectories

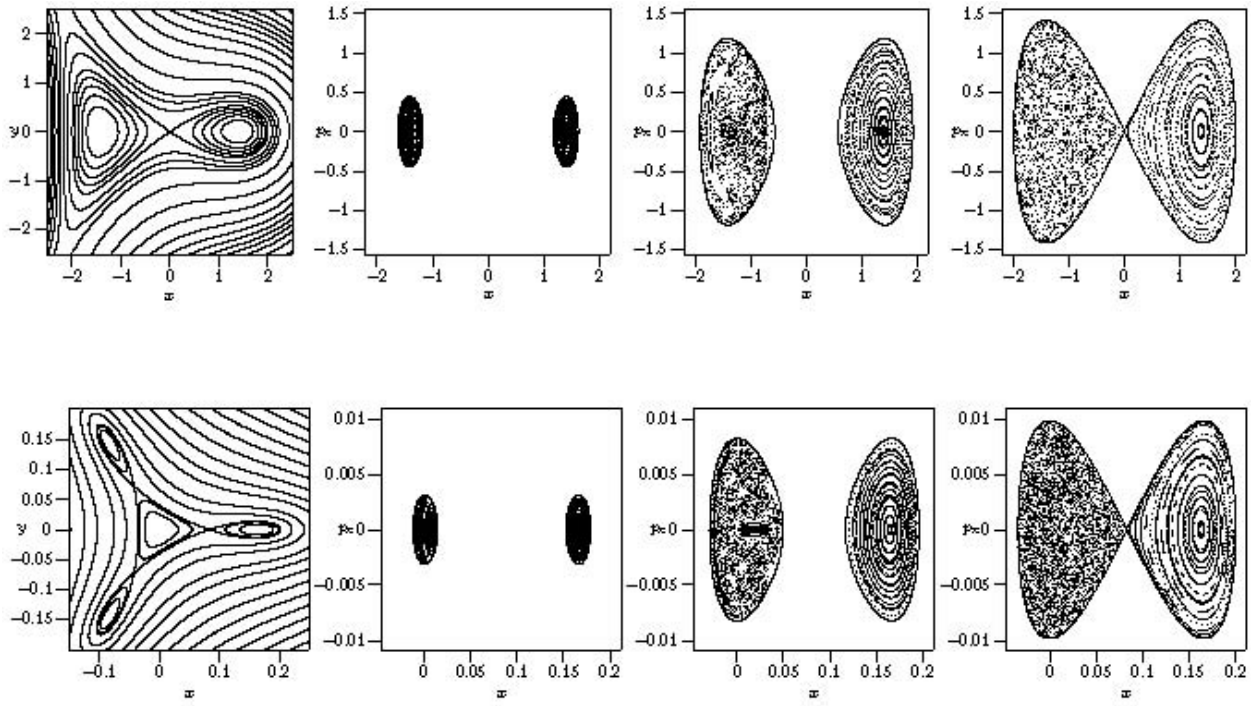

Fig. 1. Level lines and Poincaré sections for D_5 (upper row) and QO potentials at different energies under the saddle

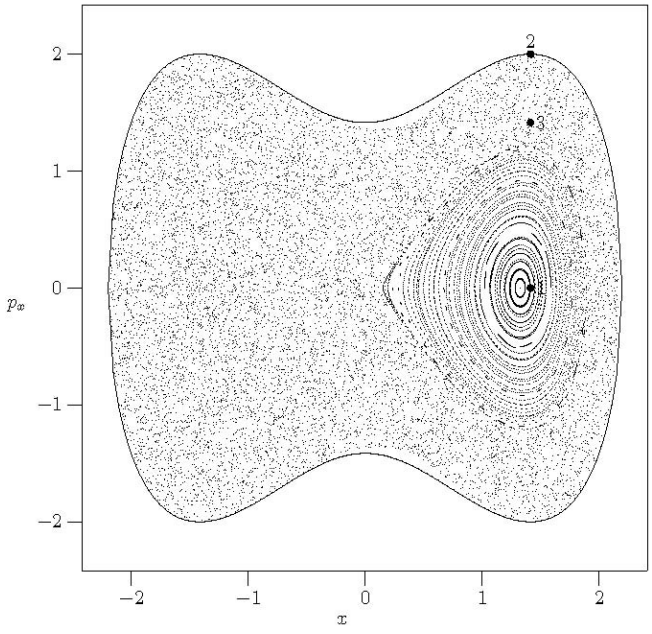

Fig. 2. Poincaré section for the D_5 potential at $E = 1.0$

could leave the well, and regular ones remain trapped, i.e. the decay of the mixed state occurs. Therefore, we will explore the escape of particles from the right well of D_5 and from peripheral wells of the QO potential.

The numerical simulation of the escape from these potentials includes three steps. At the first stage, we select an initial distribution of particles inside the well. Then the direct numerical integration of the equations of motion for all particles is performed, and we extract $N(t)/N(0)$ which is the relative number of particles in the well. Using this function, we can calculate the escape rate and a part of trapped trajectories.

One remark should be made about the first step of the numerical simulation. The initial distribution, in general, determines the ratio between regular and chaotic trajectories, and, hence, it should be physically motivated. One chance is to distribute particles uniformly in the whole classically allowed configuration space, and another one is to put all particles at the same point. The second case emulates the injection of particles to the well. In both cases, the momentum is calculated, by using the energy conservation (in the second case, it will be the same for all particles), and its direction is uniformly distributed in $[0, 2\pi]$. These initial distributions present quite simple extreme cases of real distributions. The uniform and "point" distributions will be illustrated with U_{D_5} and $U_{\rm QO}$, respectively. The phase space den-

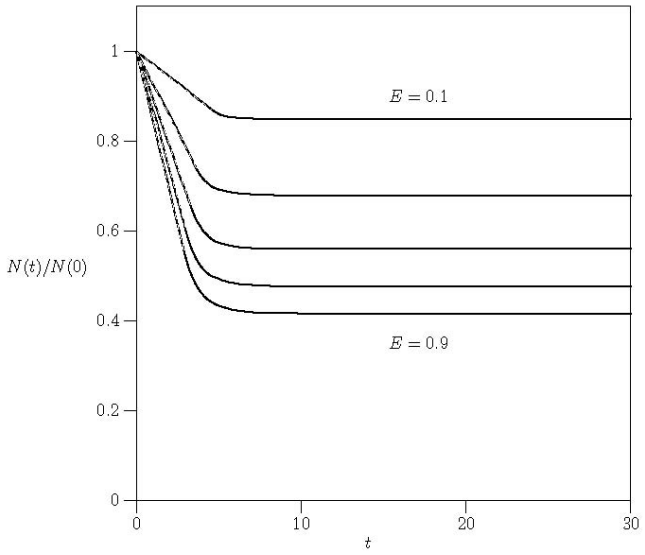

Fig. 3. Decay law $N(t)/N(0)$ for the D_5 potential at different energies. $E_i = 0.1 + 0.2k,\ k = 0 \dots 4$

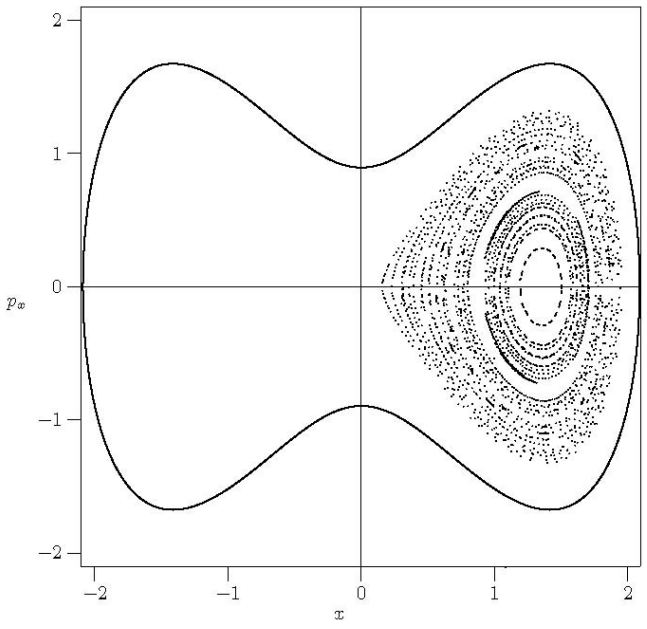

Fig. 4. Poincaré section for trapped trajectories. These trajectories form a regular island, i.e. they are regular

sity for the uniform initial distribution is

$$\rho(E) = \frac{1}{2\pi S(E)}, \tag{5}$$

where $S(E)$ is the area of the classically allowed space:

$$S(E) = \int\limits_{x>x_S} dxdy\Theta(E - U(x,y)). \tag{6}$$

The numerical simulation reveals some substantial features of the escape for this initial distribution. Figure 3 demonstrates the normalized number of particles in the well as a function of time. The decay law has three important features:
– saturation at $t \to \infty$:

$$N(t \to \infty) = \rho_\infty N_0. \tag{7}$$

Because of the uniform initial distribution, the quantity ρ_∞ is the relative phase volume occupied by trapped trajectories.
– initial linear decrease – from 0 to some $\tau(E)$:

$$N(t)/N_0 = 1 - \alpha^{(l)}t, \tag{8}$$

– exponential decrease at $t > \tau(E)$:

$$N(t)/N_0 = \rho_\infty + C\exp(-\alpha^{(e)}t). \tag{9}$$

Figure 4 presents the Poincaré section for trapped trajectories. Obviously, the regular island in the right well is formed by trapped, i.e. regular, trajectories. The function $\rho_\infty(E)$ is demonstrated in Fig. 5. This is a decreasing function, as expected from physical considerations, the number of regular trajectories decreases as the energy increases.

It is interesting to mention that there exists the correlation between $\rho_\infty(E)$ and the relative area of the regular island in the Poincaré section $\rho_{\rm PS}$. While the relative part of trapped trajectories is linked to the volume of the four-dimensional phase space occupied by regular trajectories, the Poincaré section is two-dimensional. Thus, there is no argument to expect the precise coincidence of ρ and $\rho_\infty(E)$.

To calculate the relative area of a regular island in the Poincaré section we first determine the border of the island through the numerical integration of the equation of motion and calculate the area inside it. Then this area was divided by the total area determined by the conditions $x > 0$, $p^2 > 0$. In spite of the topological nonequivalence, $\rho_{\rm PS}$ and $\rho_\infty(E)$ are very close to each other. This means that one could determine and control the part of trapped trajectories using only the Poincaré section.

The linear part of the decay law is more pronounced in comparison with a pure ensemble [10]. In the time interval between 0 and $\tau(E)$, the decay has form (8). Thus,

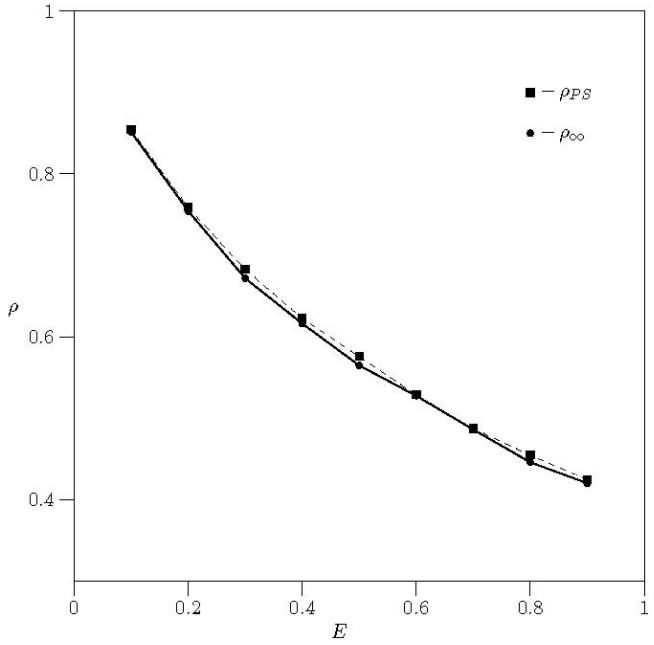

Fig. 5. Relative area $\rho_{\rm PS}$ of the regular island in the Poincaré section is shown by squares, and $\rho_\infty(E)$ is shown by circles

there are two quantities describing the linear decay: its duration $\tau(E)$ and the corresponding escape rate $\alpha^{(l)}$.

After the linear part, at $t > \tau(E)$, the decay law has exponential form (9). It is important that (8) is not a linear approximation of (9), and the linear decay has independent nature. This means that $\rho_\infty + C \neq 1$. Moreover, the decay law of form (8) precisely works up to time $t \sim \tau(E)$. In this interval, it differs substantially from the corresponding exponential law $\rho_\infty + (1-\rho_\infty)\exp(-\alpha^{(l)}t)$.

Let us now calculate $\tau(E)$. From the analysis of of the results of numerical calculations, we obtain that this time corresponds to the time of the one-dimensional, along $y = 0$, motion from the saddle to the opposite side of the well and back. Thus, $\tau(E)$ has the form

$$\tau_{D_5}(E) = 2\int\limits_0^{\sqrt{2(1+\sqrt{E})}} \frac{dx}{|v|} = \frac{\sqrt{2}}{E^{1/4}} K\left(\sqrt{\frac{1+\frac{1}{\sqrt{E}}}{2}}\right), \tag{10}$$

$$\tau_{QO}(E) = 12\left(\frac{E_S}{E}\right)^{1/4} K\left(\sqrt{\frac{1+\sqrt{\frac{E_S}{E}}}{2}}\right) =$$

$$= 6\sqrt{2}\tau_{D_5}\left(\frac{E_S}{E}\right), \tag{11}$$

where $K(k)$ is a full elliptic integral of the first type, and $E_s = 1/12^4$ is the saddle energy in the QO potential at $W = 18$.

Such a nature of $\tau(E)$ and the analysis of linearly escaping trajectories allow us to conclude that the linear decay corresponds to the escape of trajectories that move along $y = 0$ and cross the well not more than two times. Correspondingly, the trajectories which initially move toward the saddle along $y = 0$ escape firstly, and then the escape occurs for trajectories moving to the opposite part of the well.

The quantity $\alpha^{(l)}$ could be calculated via the averaging of the flow through the saddle:

$$\alpha^{(l)}(E) = \rho(E)\int\limits_{x=x_S} dy \int\limits_{-\pi/2}^{\pi/2} d\theta\,|v|\cos\theta. \tag{12}$$

This procedure is the same as in [10]. Using density (5) and integrating (12), we obtain the linear escape rate

$$\alpha^{(l)}_{D_5}(E) = \frac{E}{2\sqrt{a}S_{D_5}(E)}, \tag{13}$$

$$\alpha^{(l)}_{\rm QO}(E) = \frac{\sqrt[4]{\varepsilon}}{12\pi S_{\rm QO}(E)}\left\{(16\sqrt{\varepsilon}+1)\times\right.$$

$$\left.\times K\left(\sqrt{\frac{1-\frac{1}{16\sqrt{\varepsilon}}}{2}}\right) - 2E\left(\sqrt{\frac{1-\frac{1}{16\sqrt{\varepsilon}}}{2}}\right)\right\}. \tag{14}$$

The exponential decrease of $N(t)/N(0)$, as it could be understood from the analysis of escaped trajectories, corresponds to the leaving of sticking orbits, i.e. those chaotic trajectories which moved in a vicinity of the regular island in the Poincaré section.

The energy is a parameter which determines a part of trapped trajectories for the uniform ensemble. Changing the ensemble energy, one could trap the given number of particles.

To illustrate the splitting of the initial ensemble into the regular and chaotic components, we plot the ensemble in the (x, y) plane at a time $t \gg \tau(E)$. It is convenient to plot the asymptotic evolution of the initial ensemble in the QO potential because of the bounded character of motion in it. At $t = 0$, the particles are equally distributed between peripheral minima. Figure 6 represents this initial ensemble.

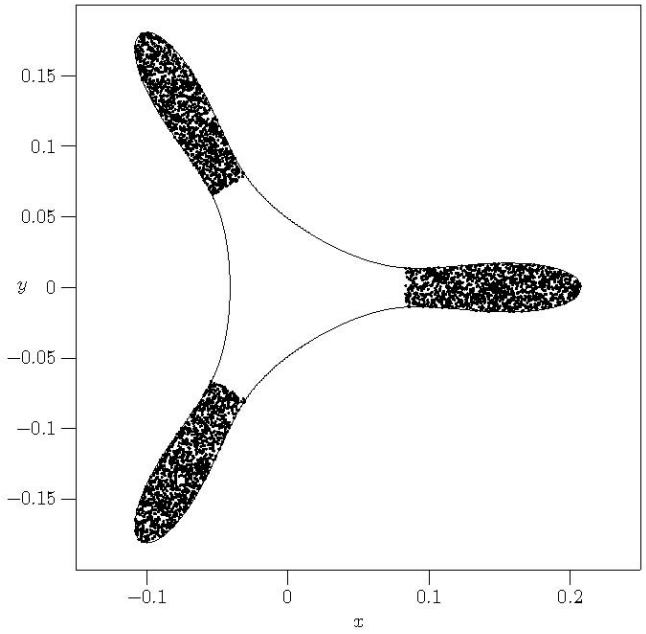

Fig. 6. Initial ensemble for the extraction of the asymptotic distribution

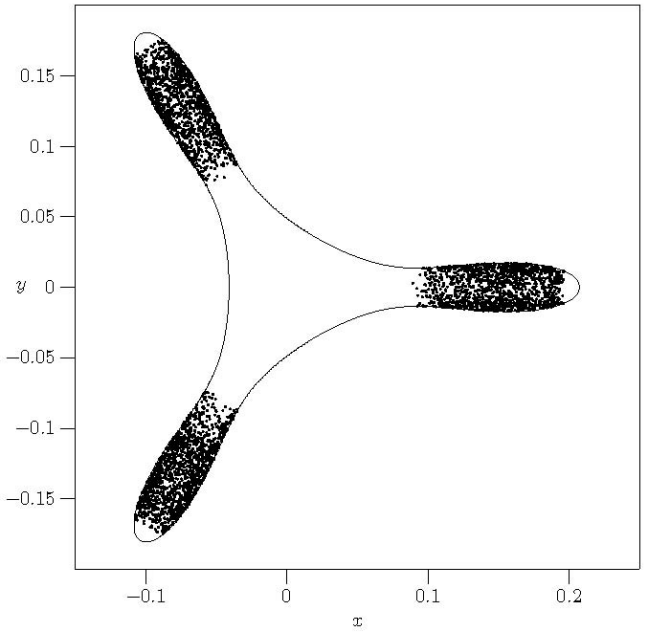

Fig. 7. Asymptotic distribution of trapped particles

The ensemble splits during the evolution in time: regular trajectories remain trapped in peripheral minima, while chaotic trajectories cover almost completely the accessible configuration space. Integrating the equations of motion for all trajectories in the initial ensemble for a enough long time (in fact – for time much greater than the typical escape time), we obtain the particles positions corresponding to the asymptotic distribution. We have calculated the asymptotic distribution for the energy $E = 1.5E_S$ ($E_S = 1/12^4$ is the saddle energy in the QO potential), while the integration was performed for $t = 150$ (for this energy, $\tau(E) = 28.395$). Figure 7 shows the asymptotic distribution of trapped particles. At an enough large time, these particles tend to accumulate closer to the center of the well.

The corresponding distribution of free particles is represented in Fig. 8. As was mentioned above, free particles cover the entire central minimum and, according to their character, the area near the line $y = 0$ in peripheral minima. Let the free particles be removed in some way. When they have left the peripheral minima (this is, of course, correct for the right well of D_5 and any well of same topology), we obtain a pure regular ensemble inside the well, i.e. the initial mixed ensemble splits.

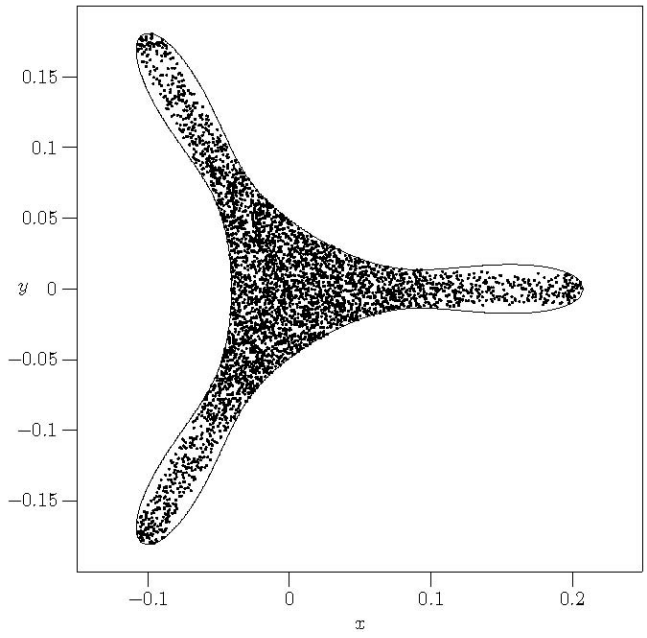

Fig. 8. Asymptotic distribution of free particles

4. Point Ensemble

For simplicity, we will consider the point distribution with $y = 0$. Thus, the governing parameter is the x_0–x–coordinate of the point of injection. The corresponding

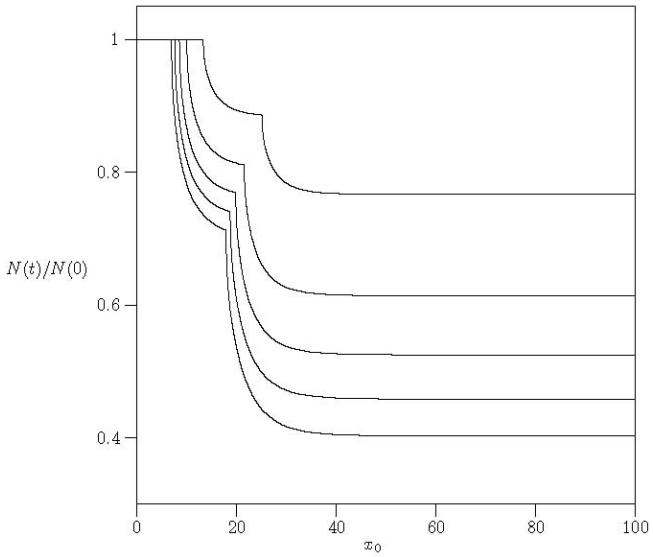

Fig. 9. Normalized particle number in the well for a point ensemble at different energies and $x_0 = 0.16$

density has the form

$$\rho\,(x, y, p, \varphi) =$$

$$= \frac{\delta\,\{x - x_0\}\,\delta\,\{y\}\,\delta\left\{p - \sqrt{2(E - U(x_0, 0))}\right\}}{2\pi\sqrt{2(E - U(x_0, 0))}}. \qquad (15)$$

The numerical procedure is identical to that for a uniform ensemble, but we can made a general conclusion about the character of decay for distribution (15) even without numerical integration.

For this, we consider the representation of an initial distribution on the Poincaré section ($y = 0$):

$$\rho_{PS}(x, p_x) = \frac{\delta(x - x_0)\Theta\left\{p_x - \sqrt{2(E - U(x_0, 0))}\right\}}{2\sqrt{2(E - U(x_0, 0))}} \times$$

$$\times\Theta\left\{\sqrt{2(E - U(x_0, 0))} + p_x\right\}, \qquad (16)$$

where $\Theta\,\{a\}$ is a step function. Let us denote

$$p_x^{(\max)} = \sqrt{2(E - U(x_0, 0))}. \qquad (17)$$

Thus, in the Poincaré section, the initial ensemble occupies the interval $x = x_0, p_x \in \left[-p_x^{(\max)}, p_x^{(\max)}\right]$. The edges of this interval correspond to the momentum directions $\varphi = \pi, 0$. In the over-barrier case, this interval crosses the regular island at the points $(x_0, p_x^{(\mathrm{reg})})$ and $(x_0, -p_x^{(\mathrm{reg})})$. Obviously, the particles with p_x in the interval $\left[-p_x^{(\mathrm{reg})}, p_x^{(\mathrm{reg})}\right]$ could not leave the well. The quantity

$$\varphi_{\max}(E, x_0) = 2\arccos\left(\frac{p_x^{(\mathrm{reg})}}{p_x^{(\max)}}\right) \qquad (18)$$

defines the cone of directions, along which the particles can leave the well. In other words, the particles with p_y which is greater than some maximum value are trapped. Thus, the first conclusion about the decay of a point ensemble implies the existence of the escape cone, and this feature reveals the role of transversal momenta in the escape.

The second feature consists in the fact that the decay begins at the time τ_1 which corresponds to the time of motion of a particle with momentum $p_x = -p$ from the point x_0 to the saddle:

$$\tau_1 = \int\limits_{x_S}^{x_0} \frac{dx}{p_x} = \int\limits_{x_S}^{x_0} \frac{dx}{\sqrt{2(E - U(x, 0))}}. \qquad (19)$$

Moreover, the escape is a two-stage process due to the existence of the escape cone. At the second stage, the particles moving toward the well boundary in the escape cone leave the well.

The numerical procedure implies the determination of $\varphi_{\max}(x_0, E)$, $\tau_1(x_0, E)$, and $N(t = \infty)$, i.e. the number of particles in the well. Due to the uniform distribution of the directions of momenta, we have the relation

$$\rho_\infty(x_0, E) \equiv \frac{N(\infty)}{N(0)} = 1 - \frac{\varphi_{\max}(x_0, E)}{\pi}. \qquad (20)$$

We will illustrate the above consideration for the QO potential. The energy is normalized to the saddle energy, $E_S = 1/144^2$: $E = \varepsilon E_S$. The initial ensemble is localized in a peripheral minimum with $x_{\min} = 1/6$, and the corresponding saddle $x_S = 1/12$. Figure 9 represents the normalized number of particles in the well as a function of the time for different values of the energy and $x_0 = 0.16$.

Numerically obtained τ_1 can be compared to the analytical value

$$\tau_1 = \int\limits_{1/12}^{x_0} \frac{dx}{p_x} = \int\limits_{1/12}^{x_0} \frac{dx}{\sqrt{2(\varepsilon E_S - U_{\mathrm{QO}}(x, 0))}}. \qquad (21)$$

The numerical and analytical values of the first escape time are presented in Fig. 10.

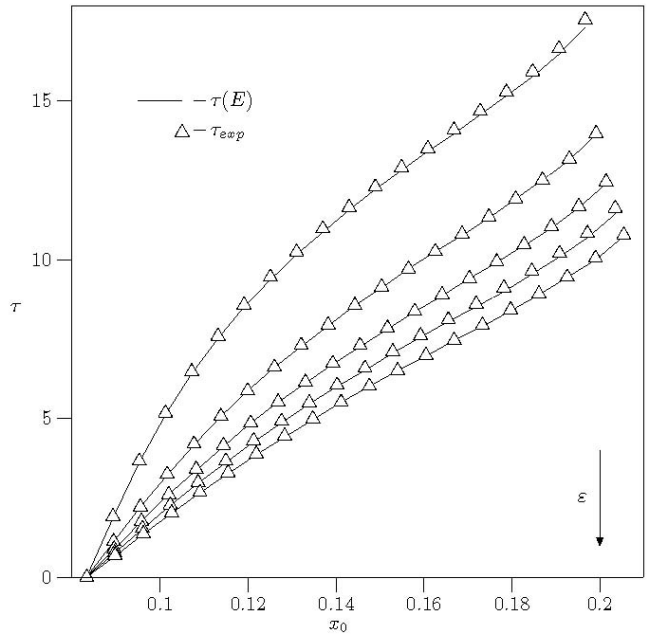

Fig. 10. First escape time τ_1; $\tau_{\exp}$ – obtained numerically, $\tau(E)$ – calculated analytically

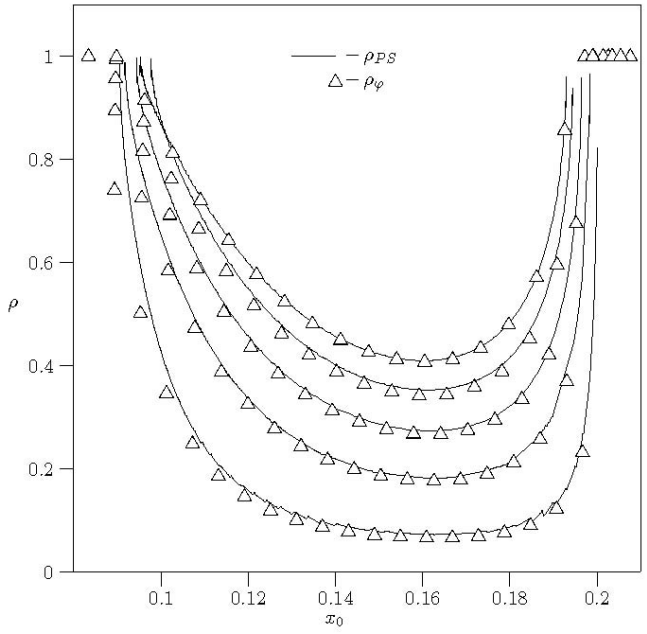

Fig. 11. $\rho_{\rm PS}$ and ρ_φ for different energies and injection points

The most interesting question is the correspondence between the escape cone angle, the number of trapped particles, and a linear part of the regular island in the Poincaré section. Figure 11 represents the quantities

$$\rho_{\rm PS} = 1 - \frac{p_x^{(\rm reg)}(x,\varepsilon)}{p_x^{(\rm max)}(x,\varepsilon)} \tag{22}$$

and

$$\rho_\varphi = 1 - \cos(\varphi_{\max}(x,\varepsilon)/2). \tag{23}$$

The first quantity is a linear part of the regular island in the section, and second one is the corresponding expression through the escape cone angle.

This angle could be determined by a numerical simulation. Thus, the Poincaré section can be used to determine the angle of the escape cone. On the other hand, this angle is related to the part of trapped trajectories. To demonstrate this connection, we compare

$$\rho_\varphi^{(N)} = 1 - \frac{\varphi_{\max}(x,\varepsilon)}{\pi} \tag{24}$$

with ρ_∞. The corresponding data are presented in Fig. 12. This analysis allows us to conclude that the point ensemble differs substantially from the uniform one, when considering the escape.

In a uniform ensemble, the Poincaré section gives only an estimate (nevertheless, very accurate) of the number of trapped particles. In the point ensemble, one

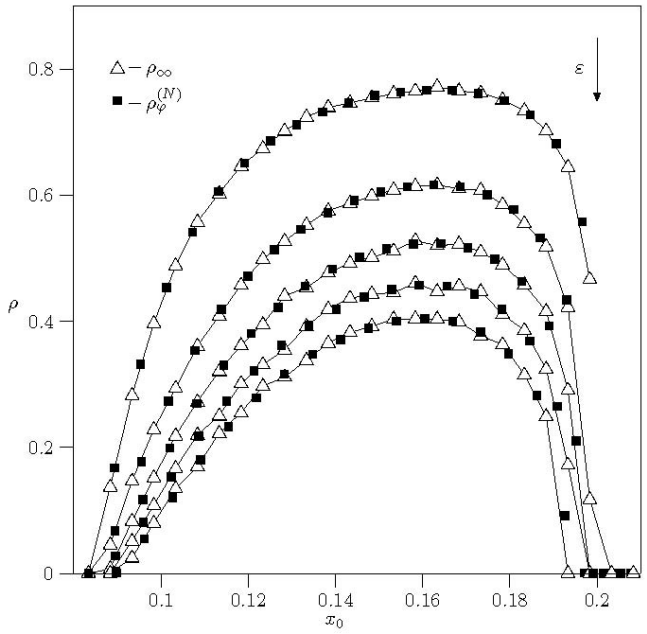

Fig. 12. ρ_∞ and $\rho_\varphi^{(N)}$ for different energies and injection points

can calculate not only a part of trapped particles, but also the escape cone angle, using only the Poincaré section. The point ensemble allows a dual control of the part of trapped particles, using the energy and the injection point. We even should not compute the entire Poincaré section, but only the boundary of the regular

island, $p_x^{(\mathrm{reg})}(x_0, \varepsilon)$, and then we can use the relation

$$\rho_\infty = 1 - \frac{2 \arccos\left(\frac{p_x^{(\mathrm{reg})}}{p_x^{(\mathrm{max})}}\right)}{\pi}. \qquad (25)$$

The procedure of calculation of the part of trapped particles, thus, includes three steps. First of all, we need to calculate the boundary of the regular island in the Poincaré section. After that, the $p_x^{(\mathrm{reg})}$ and $p_x^{(\mathrm{max})}$ should be determined. Now the value ρ_∞ can be calculated.

5. Conclusions and Future Research

We have studied the escape from localized areas of the configuration space under the existence of a mixed state. When the mixed state is present in the system, it is possible to "trap" a given number of particles in the well. We have considered two possible initial distributions.

For the uniform distribution, the escape law splits into three sections. The first and second sections correspond to the linear and exponential decays, respectively, and the third section is characterized by a plateau which corresponds to trapped particles. The number of trapped particles depends only on the energy.

In the case of a point ensemble, the escape is a two-stage process, and the number of trapped particles depends not only on the energy, but on the coordinate of the injection point too. Only trajectories with directions of initial momenta in some cone can escape. The escape cone angle is related to the linear part of the regular island in the Poincaré section and the number of trapped trajectories. Moreover, only the edge of the regular island is required to compute the number of trapped particles.

The natural question arises about whether the considered features of the escape problem in potentials with a mixed state preserve under the influence of weak noise and friction. The integration of the Langevin equation is the obvious method to answer this question. However, the numerical integration of stochastic differential equations with chaotic potential leads to some complications: the low-order methods give too large errors due to a strong dependence on initial conditions, whereas the more advanced algorithms are computationally expensive. Nevertheless, this is an important topic for researches. Moreover, the analytical estimations of the escape rate can be performed not only by using the well-known Kramers approach, but by considering the connection between the Fokker–Planck equation and quantum mechanics. Algorithms for a numerical solution of the Schrödinger equation are more robust, the corresponding quantum problem, being solved, provides a solution of the Fokker–Planck equation. The recent results in $N = 4$ supersymmetric quantum mechanics ($N = 4$ SUSYQM) [16] boost the procedure even further: one can not only construct the quantum Hamiltonian for the considered stochastic system, but also additional Hamiltonians which are related to new stochastic processes. Although analytically intensive, the procedure of construction of new Hamiltonians and, thus, new stochastic systems is straightforward and very promising, by presenting the important information about escape, e.g., its rate.

1. Yu. Bolotin, A. Tur, and V. Yanovsky, *Chaos: Concepts, Control and Constructive Use* (Springer, Berlin, 2009).
2. W.C. Sabine, *Collected Papers on Acoustics* (Harward Univ. Press, Cambridge, 1922).
3. O. Legrand and D. Sornette, Phys. Rev. Lett. **66**, 2172 (1991).
4. L.A. Bunimovich and C.P. Dettmann, arXiv:nlin/0610013.
5. W. Bauer and G.F. Bertsch, Phys. Rev. Lett. **65**, 2213 (1990).
6. H. Alt *et al.*, Phys. Rev. E **53**, 2217 (1996).
7. V. Kokshenev and M. Nemes, Physica A **275**, 70 (2000).
8. L.A. Bunimovich, C.P. Dettmann, Phys. Rev. Lett. **94**, 100201 (2005).
9. H.E. Kandrup, C. Ciopis, G. Coutopoulos, and R. Dvorak, arXiv:astro-ph/9904046
10. H.J. Zhao and M.L. Du, arXiv:nlin.CD/0701028
11. J. Aguirre, *Uncertainty in Nonlinear Dynamics: Fractal Structures, Celullar Models and Control of Chaos, Ph.D. thesis* (2003).
12. Yu.L. Bolotin , V.A. Cherkaskiy, and G.I. Ivashkevych, Phys. Lett. A **372**, 4080 (2008).
13. V.P. Berezovoj, Yu.L. Bolotin, V.A. Charkaskiy, and G.I. Ivashkevych, *Regular and Chaotic Classical and Quantum Dynamics in Multiwell Potentials* (Cambridge Sci. Publ., Cambridge, 2009) (in press).
14. Yu.L. Bolotin, V.Yu. Gonchar, and E.V. Inopin, Yad. Fiz. **45**, 351 (1987).
15. V.P. Berezovoj, Yu.L. Bolotin, and V.A. Cherkaskiy, Phys. Lett. A **323**, 318 (2004).
16. V.P. Berezovoj, G.I. Ivashkevych, and M.I. Konchatnij, Phys. Lett. A **374**, 1197 (2010).

Received 21.01.10

НАДБАР'ЄРНИЙ РОЗПАД ЗМІШАНОГО СТАНУ
У ДВОВИМІРНИХ БАГАТОЯМНИХ ПОТЕНЦІАЛАХ

Ю.Л. Болотін, В.О. Черкаський, Г.І. Івашкевич, А.І. Кірдін

Р е з ю м е

Проведено аналітичні та чисельні дослідження класичного вильоту у двовимірних гамільтонових системах зі змішаним станом. У потенціалах, в яких існує змішаний стан, тобто фазовий простір містить одночасно області регулярного та хаотичного руху, задача вильоту має низку нових властивостей. Зокрема, деякі локальні мінімуми перетворюються на пастки, число частинок у яких залежить від енергії та інших величин, що характеризують ансамбль частинок. Початкова форма ансамблю задає набір параметрів, що визначають число захоплених частинок.